Alexandria Engineering Journal 106 (2024) 367–379

Contents lists available at ScienceDirect

Alexandria Engineering Journal

journal homepage: www.elsevier.com/locate/aej

Original article

Influence of rotating magnetic field on thermal field and entropy generation of a tube containing the nanofluid using mixture model

Mohammad Hossein Razavi Dehkordi [a,b], Noushin Azimy [c], Shahab Naghdi Sedeh [d], Hamidreza Azimy [a], Seyed Amir Mohammad Ahmadi [e], Mohammad Akbari [a,b,*]

[a] Department of Mechanical Engineering, Najafabad Branch, Islamic Azad University, Najafabad, Iran
[b] Aerospace and Energy Conversion Research Center, Najafabad Branch, Islamic Azad University, Najafabad, Iran
[c] Department of Mechanical Engineering, Engineering Faculty, Shahid Chamran University of Ahvaz, Ahvaz, Iran
[d] Department of Mechanical Engineering, Mobarakeh Branch, Islamic Azad University, Mobarakeh, Iran
[e] Department of Mechanical Engineering, Shahinshahr Branch, Islamic Azad University, Shahinshahr, Iran

ARTICLE INFO

Keywords:
Nanofluid
Magnetic field
Mixture model
Entropy generation

ABSTRACT

The thermo-fluidic properties and entropy generation in a tube comprising nanofluid under variable rotational magnetic field have not been studied earlier. In the current study, the influence of a rotating magnetic field is evaluated by using mixture model at four different pump power for three cases. A steady-state, Newtonian Ag/water nanofluid, incompressible, and 3D model have been supposed. The influence of pump power variation and using nanofluid are studied. Results indicated that by raising the pump power for three cases, the Nusselt number enhances, and Bejan number, the friction factor, and dimensionless temperature decreases. The rotating magnetic field for the Case III in comparison to the Case I and Case II at 60 W and 0.5 % volume fraction of nanofluid, enhanced the Nusselt number by 356.3 % and 12.42 %, respectively. In the presence of 0.5 % nanofluid at 60 W pump power, the friction factor increases by 103.5 % compared to Case I, with the same fluctuations observed in Cases II and III. The maximum dimensionless temperature reached 0.575 for Case III at a power of 30 W using water. A rotating magnetic field of 60 W raised PEC by 219.44 % and 261.11 % for Cases II and III, respectively, compared to Case I.

1. Introduction

Thermal field and entropy generation are important concepts in the field of thermodynamics, which are essential in understanding the behavior of fluids and their interactions with their surroundings [1–4]. With the advancement of technology, researchers have been exploring new ways to enhance the heat transfer capabilities of fluids, leading to the development of nanofluids. The study of nanofluids, which are fluids containing suspended nanoparticles, has gained significant attention in recent years due to their potential applications in various fields, such as heat transfer, manufacturing, energy storage, and biomedicine [5–9]. These are suspensions of nanoparticles in a base fluid, which have shown promising results in improving thermal performance. Also, one area of research that has been of particular interest is the influence of a magnetic field on the thermal field and entropy generation of the nanofluids [10–14]. In the science of heat transfer, magnetic nanofluids, a novel kind of heat transfer medium, have garnered a lot of interest since they offer a potential path to low energy consumption and carbon neutrality [15]. Fan et al. [16] carried out an empirical analysis on the particle fouling qualities of magnetic Fe_3O_4-H_2O-AG nanofluids in order to completely discuss the viability of their application in heat exchange systems. On the fouling characteristics, the effects of several factors were examined. The outcomes indicated that a high Reynolds number, a static parallel magnetic field (MF) with a higher flux density, and a tube with a twisted turbulator illustrate lower fouling thermal resistance. Mousavi et al. [17] utilized the finite volume method (FVM) with the SIMPLEC algorithm to explore the impact of a magnetic field variation on the thermal behavior of a sinusoidal double pipe heat exchanger (HE) including Fe_3O_4 nanofluid. Results reveal that diffusion improves as the magnetic field intensity enhances. Bezaatpour and Goharkhah [18] presented an innovative strategy to decrease the pressure drop and enhance the convective heat transfer in a double-pipe HE under a MF. Results indicate that the MF raise heat transfer up to 320 % with a little enhancement in pressure drop. Shakiba and Vahedi [19] analyzed the hydro-thermal characteristics of Fe_3O_4 in a double pipe HE in the

* Corresponding author at: Department of Mechanical Engineering, Najafabad Branch, Islamic Azad University, Najafabad, Iran.
E-mail address: m.akbari.g80@gmail.com (M. Akbari).

https://doi.org/10.1016/j.aej.2024.07.012
Received 8 October 2023; Received in revised form 16 March 2024; Accepted 3 July 2024
Available online 13 July 2024

Nomenclature

D_h	The hydraulic diameter of the tube (m)
k	Thermal conductivity (W/m. K)
h	Heat transfer coefficient (W/m^2. K)
f	Friction factor
L	Length (mm)
U	Non-dimensional velocity
Be	Bejan number
r_0	Tube radius
q	Heat Flux (W)
C_p	Specific heat (J/kg. K)
P	Pressure (Pa)
T	Temperature (℃)
u_i	Mean velocity components in the x_i direction (m/s)
x_i	Cartesian coordinates (m)
T_b	Bulk temperature (K)
T_w	Wall temperature (K)
Nu	Nusselt number
B_0	Magnetic field strength (T)
$S'''_{gen,T}$	Thermal entropy generation
$S'''_{gen,F}$	Frictional entropy generation
$S'''_{gen,M}$	Entropy generation generated by magnetic field
ΔP	Pressure drop (Pa)

Greek Symbols

θ	Dimensionless temperature
μ	Dynamic molecular viscosity
ρ	Density (kg/m3)
φ	Volume Fraction (%)
Ω	Pump power (W)
ω	Rotational velocity
σ	Electrical Conductivity (Ω. m)-1

Subscripts

nf	Nanofluid
np	Nanoparticle
f	Fluid
m	Mixture

presence of a non-uniform lateral MF with variable intensities. It is concluded that a non-uniform lateral MF is able to control the flow of nanofluid and enhance the heat transfer ratio of a double pipe HE. Ma et al. [20] analyzed the thermal behavior of thermo-gravitational convection in a shell and tube HE using Fe_3O_4/water nanofluid under MF effect. Based on their study, the energy transport rate indicates an inverse relation with the Ha number, however, a direct dependency with the MF tilt angle.

Hosseinizadeh et al. [21] studied the performance of the HE comprising a triple tube under a uniform MF at different configurations. It is indicated that employing a MF is impressive for raising the heat transfer rate and the triple tube heat exchanger efficiency. In Azizi et al.'s [22] research, the utilization of the non-uniform MF on the rate of heat transfer of double tube HE with various geometries containing nanofluids is comprehensively investigated. The outcomes reveal that the magnetic source amplifies the rotation flow in the slit of the inner tube, and consequently, heat transfer is enhanced in the area. Sodagar-Abardeh et al. [23] investigated laminar incompressible flow and combined convection in a space under an axial MF. The outcomes show that an enhancement in the Ha number reduces the average local Nu number. Chu et al. [24] utilized FVM to numerically investigated the thermos-fluid characteristics through the 180˚ elbow pipe under a non-uniform MF. Their findings indicate enhancing the magnetic intensity raises the average Nusselt number to 30 %. Alnaqi et al. [25] investigated the impacts of MF and radiation on the entropy generation and heat transfer rate in a cavity with a conductor fin. It was also found that enhancing the radiation parameter at higher Ra numbers enhances the entropy generation and Nu number and reduces the Bejan number. Hosseini and Sheikholeslami [26] evaluated the thermal efficiency and thermodynamics law in a microchannel under a MF. Based on their results, involving magnetic field decreases the entropy generation. Selimefendigil and Oztop [27] numerically studied the natural convection in a cavity comprising various shaped obstacles under the result of a uniform MF and uniform heat using nanofluids. With rising Ha number values, the impact of heat transfer reduces with two shapes of obstacles compared to the case without obstruction is less impressive. Bahiraei and Hangi [28] used the two-phase method to examine the behavior of a water-based Mn-Zn magnetic nanofluid in double-pipe HE in a quadrupole MF. In their study, the impact of magnetic force is decreased at higher Re numbers. Khetib et al. [29] investigated the entropy generation and natural convection in the enclosure under a MF and radiation impacts using MgO/Water nanoliquids. Additionally, any modifications to the enclosure angle and MF had a variety of consequences on the heat transition. According to the findings, increasing the size of the blade first increased and then decreased the heat transition ratio and generated entropy. Last but not least, raising the fin always raised the Be. Heat transition of the magnetic nanoliquid in a tube under a non-uniform MF is studied by Hariri et al. [30]. Results reveal that Nusselt number enhances under the MF. Also, diffusion increases by enhancing the volume fraction of Fe_3O_4 nanoparticles. Safarzadeh et al. [31] estimated entropy generation in a helically coiled tube utilizing micro-fin tube under the MF. For water and nanoliquid, respectively, the helically coiled tube with diameters of 90 and 135 mm are the best cases from an energy standpoint among the other coils at a set pitch.

Chamkha et al. [32] evaluated the natural convection and entropy generation in a C-shaped cavity containing CuO-water nanofluid under a uniform MF. It is discovered that the used MF can reduce the rate of both entropy generation and natural convection, with the reduction in total entropy generation for Ra = 1000 and = 0.04 decreasing from 96.27 % to 48.17 % for Ha = 45 when the aspect ratio is raised from 0.1 to 0.7. Shah et al. [33] analyzed the entropy optimization of a hybrid nanoliquid inside a wavy cavity under an ambient constant MF. The medium porosity and increasing Lorentz forces cause the Bejan number to increase. With increasing buoyancy forces and mild porosity, the average Nu number raises while falling with a stronger MF. Numerical research is done by Selimefendigil et al. [34] on the mixed convection of CuO/-water nanoliquid in an enclosure with upper and lower triangular areas under the influence of inclined MF. It has been found that when the triangular domains' Richardson and Ha numbers raise, the local and averaged heat transfer deteriorates. In comparison to the lower triangular region, the averaged transfer degrades more as the Ha number and magnetic angle of the top triangle grow. Aydın et al. [35] experimentally analyzed the magnetic flux density of $NiFe_2O_4$ nanoparticles concentration in water on the thermal behavior of a heat pipe. The highest increment in the heat pipe's thermal resistance was derived as 30.4 %, by $NiFe_2O_4$/water nanoliquid utilization under a MF.

Pour Razzaghi et al. [36] evaluated the thermal performance and irreversibilities in LS-3 solar collector equipped with the rotary twisted tape and exposed the line dipole magnetic field. Dipole magnetic field enhances convective heat transfer coefficient (CHTC) over 97 % at B = 100 G. Selimefendigil and Oztop [37] evaluated the impact of a tilted MF and porous cylinders in a cavity using Finite Element Method (FEM). The numerous cylinders with the maximum permeability show an average heat transfer variance of up to 19.8 %. In laminar flow with

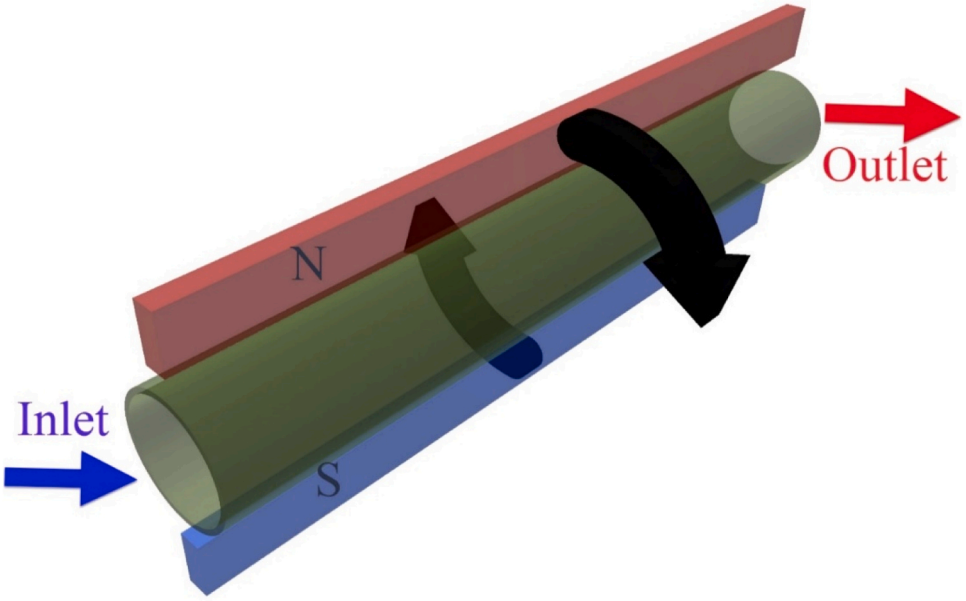

Fig. 1. Proposed geometry of the investigation.

subjected to permanent MFs, Mehrali et al. [38] examined the thermos-fluid characteristics of hybrid graphene-magnetite nanoliquids. The experimental findings showed that, in the absence of a MF, the heat transfer enhancement of hybrid magnetite nanoliquid over distilled water was minimal. Moreover, under a MF, the characteristics of heat transport have greatly enhanced. Pordanjani et al. [39] looked into the impact of radiation on the rate of CHTC and the creation of nanofluid entropy in a diagonal, rectangular chamber with a MF. The findings indicate that as the Ra number increases and the Ha number lowers, the Nu number and entropy generation raise while the Bejan number falls. The Bejan number raises while the heat transfer rate and entropy formation decrease as the MF's angle is increased. In a curved tube with a MF, Aminfar et al. [40] demonstrated the impact of a MF on the mixed convection. Based on the findings, the CHTC may be improved by utilizing a tube with curves rather than a straight tube, adding nanoparticles with magnetic properties to the base fluid, and generating an external MF. It is determined that heat transition is improved owing to secondary flow enhancement and thermal conductivity enhancement.

The thermos-fluid entropy generation and characteristics in a tube contained nanofluid under a variable rotating MF has not been studied so far. Due to its potential applications in physics, medical science, and engineering, the current research studies the impact of a rotating MF at three dimensionless velocities, i.e., Case I: static uniform magnetic field; Case II: rotating magnetic field with constant dimensionless velocity; and Case III: rotating magnetic field with twice the velocity of Case II, on a tube including Ag/water nanofluid. In this study for the first time, an incremental rotating magnetic field has been applied to a tube and its effect on Be, f, Nu, θ and PEC has been investigated. Looking at past studies, we find that most of the previous works were done in two dimensions and with simplifying assumptions [41–43]. The idea of magneto-hydrodynamics that stems from managing thermal behavior or controlling the viscosity property of liquids is what piques interest in these challenges. Examples in the metallic processing industry include liquid metal control in continuous casting, plasma welding, electrolytic hall cells for aluminum smelting, electromagnetically supported melts, and many more. Magneto science also covers the application of the magnetic field in medical science. Presently, instead of the previously available medicine, which has negative effects, exposing a person to a magnetic field may enhance blood flow throughout their body. The experiment in the hostile environment found in any of these applications is extremely tough to complete [44]. The thermodynamics' first and second laws are estimated using the two-phase model.

Table 1
The nanoparticles' thermophysical properties [45,46].

	Heat capacity (J. kg^{-1}. K^{-1})	Viscosity (kg. m^{-1}. s^{-1})	Density (kg. m^{-3})	Electrical Conductivity $(\Omega.m)^{-1}$	Thermal conductivity (W. m^{-1}. K^{-1})
Ag	235	-	10500	6.3×10^{7}	429
Water	4179	0.003001	997.1	5.5×10^{-5}	0.613

2. Numerical model

The proposed geometry is demonstrated in Fig. 1.
The considered assumptions for this simulation are listed below.

2.1. Assumptions

- A steady-state, Newtonian Ag/water nanofluid, incompressible, and 3D model have been supposed.
- Ag/water nanofluid has been considered as the working fluid.
- No temperature jumps in boundaries was assumed.
- The solution conducted by Pressure Based solver.

Additionally, the thermal and physical properties of the proposed Ag nanoparticles and water base fluid are mentioned in Table 1.

2.2. Governing equations and measurements parameters

In base fluid, nanoparticle distribution is thought to be homogeneous. The governing equations are as follows:

Continuity equation [47,48]

$$\frac{\partial u_i}{\partial x_i} = 0 \tag{1}$$

Where u is flow velocity (m/s).

Momentum equation [49]

$$\frac{\partial u_i u_j}{\partial x_i} = \frac{1}{\rho}\frac{\partial P}{\partial x_i} + \frac{\partial}{\partial x_i}\left((\nu - \nu_t)\left(\frac{\partial u_j}{\partial x_i} - \frac{\partial u_i}{\partial x_j}\right)\right) + \omega\frac{\partial B_0}{\partial x_i} \tag{2}$$

Where is υ is kinematic viscosity (m/s^2), ρdensity (kg/m^3), B_0 is magnetic field (T), P is pressure (Pa), and ω is rotational velocity (rad/s).

Energy equation [49]

$$\frac{\partial u_i T}{\partial x_i} = \frac{\partial}{\partial x_i}\left(\left(\frac{\nu}{\mathrm{Pr}} + \frac{\nu_t}{\mathrm{Pr}_t}\right)\frac{\partial T}{\partial x_i}\right) \tag{3}$$

Where T and Pr are temperature (K) and Prandtl number, respectively.

Turbulent kinetic energy [49]

$$\frac{\partial}{\partial x_i}\left[\rho k u_j\right] = \frac{\partial}{\partial x_j}\left(\left(\mu + \frac{\mu_t}{\sigma_k}\right)\frac{\partial k}{\partial x_j}\right) + G_k + G_b - \rho\varepsilon + Y_M + S_k \tag{4}$$

Turbulent dissipation rate [49]

$$\frac{\partial}{\partial x_i}\left[\rho\varepsilon u_j\right] = \frac{\partial}{\partial x_j}\left(\left(\mu + \frac{\mu_t}{\sigma_k}\right)\frac{\partial \varepsilon}{\partial x_j}\right) + \rho C_1 S_\varepsilon + \rho C_2 \frac{\varepsilon}{k + \sqrt{\nu\varepsilon}} + C_{1\varepsilon}\frac{k}{\varepsilon}C_{3\varepsilon}G_b + S_\varepsilon \tag{5}$$

Where:

$$\mu_t = \rho C_\mu \frac{k^2}{\varepsilon} \tag{6}$$

$$G_k = \mu_t S^2 \tag{7}$$

$$G_b = -\frac{1}{\rho}\left[\frac{\partial P}{\partial T}\right]_P g_i \frac{\mu_t}{0.85}\frac{\partial T}{\partial x_i} \tag{8}$$

$$Y_M = 2\rho\varepsilon\frac{k}{\gamma RT} \tag{9}$$

$$C_1 = \max\left(0.43, \frac{\eta}{\eta + 5}\right) \tag{10}$$

$$S = \sqrt{2S_{ij}S_{ij}} \tag{11}$$

$$k = \frac{3}{2}u_{ave}^2 I^2 \tag{12}$$

$$\varepsilon = \rho C_\mu \frac{k^2}{\mu}\left[\frac{\mu_t}{\mu}\right]^{-1} \tag{13}$$

$$I = 0.1\mathrm{Re}_{in}^{-\frac{1}{8}} \tag{14}$$

$$C_{1\varepsilon} = 1.44 - C_2 = 1.9 - \sigma_k = 1 - \sigma_\varepsilon = 1.2$$

Where K, ε, u_{avg}, I, S, μ_t, and C_μ are inlet turbulent kinetic energy, turbulence dissipation rate, mean velocity of the flow, the turbulence intensity, user-defined source terms, turbulent kinetic viscosity, and empirical constant value which is about 0.09, respectively.

The thermal properties are as follows [50]:

$$h(x) = \frac{q''(x)}{(T_w(x) - T_b)} \tag{15}$$

$$T_w(x) = \frac{1}{A}\int T dA \tag{16}$$

$$T_b(x) = \frac{\int T\rho|VdA|}{\int \rho VdA} \tag{17}$$

$$h = \frac{1}{L}\int_0^L h(x)dx \tag{18}$$

$$\theta = \frac{T_f - T_b}{T_w - T_b} \tag{19}$$

Where h(x) is local convection heat transfer coefficient, T_w is wall temperature, T_f is fluid temperature, T_b is fluid bulk temperature, h is average convection heat transfer coefficient, and θ is dimensionless temperature.

Also, friction factor is expressed as follow [50]:

$$f = \frac{2\Delta p D_h}{L\rho V_{in}^2} \tag{20}$$

And the local average Nu number is defined as mentioned below [50]:

$$Nu = \frac{hD_h}{K_{nf}} \tag{21}$$

The frictional entropy generation, thermal entropy generation, and MF entropy generation defined as follows [50]:

$$S'''_{gen,F} = \frac{\mu_{nf}}{T}\phi \tag{22}$$

$$S'''_{gen,T} = \frac{k_{nf}}{T^2}(\nabla T)^2 \tag{23}$$

$$S'''_{gen,M} = \frac{\sigma_{nf}B_0^2 u^2}{T} \tag{24}$$

Eq. (25) presents the proportion of entropy generation due to the heat transfer per the overall entropy generation that is Bejan number [50]:

$$Be = \frac{S'''_{gen,T}}{S'''_{gen,T} + S'''_{gen,F} + S'''_{gen,M}} \tag{25}$$

And the Performance Evaluation Criterion (PEC) [51]:

$$PEC = \frac{Nu/Nu_b}{(f/f_b)^{\frac{1}{3}}} \tag{26}$$

The thermal properties of the proposed nanofluid are evaluated from Eqs. (27)-(30) [46,51]:

- Dynamic viscosity:

$$\mu_m = \frac{\mu_f}{(1-\varphi)^{2.5}} \tag{27}$$

- Density:

$$\rho_m = (1-\varphi)\rho_f + \varphi\rho_{np} \tag{28}$$

- Thermal conductivity:

$$k_m = k_f\left[1 + 2.72\varphi + 4.97\varphi^2\right] \tag{29}$$

- Specific heat capacity:

$$(\rho C_p)_m = \left(1-\varphi\right)(\rho C_p)_f + \varphi(\rho C_p)_{np} \tag{30}$$

- Electrical Conductivity:

$$\frac{\sigma_{nf}}{\sigma_f} = 1 + \frac{3\left(\frac{\sigma_s}{\sigma_f} - 1\right)\varphi}{\left(\frac{\sigma_s}{\sigma_f} + 2\right) - \left(\frac{\sigma_s}{\sigma_f} - 1\right)\varphi} \tag{31}$$

To obtain the non-dimensional velocity parameter, the following formulation is used [52]:

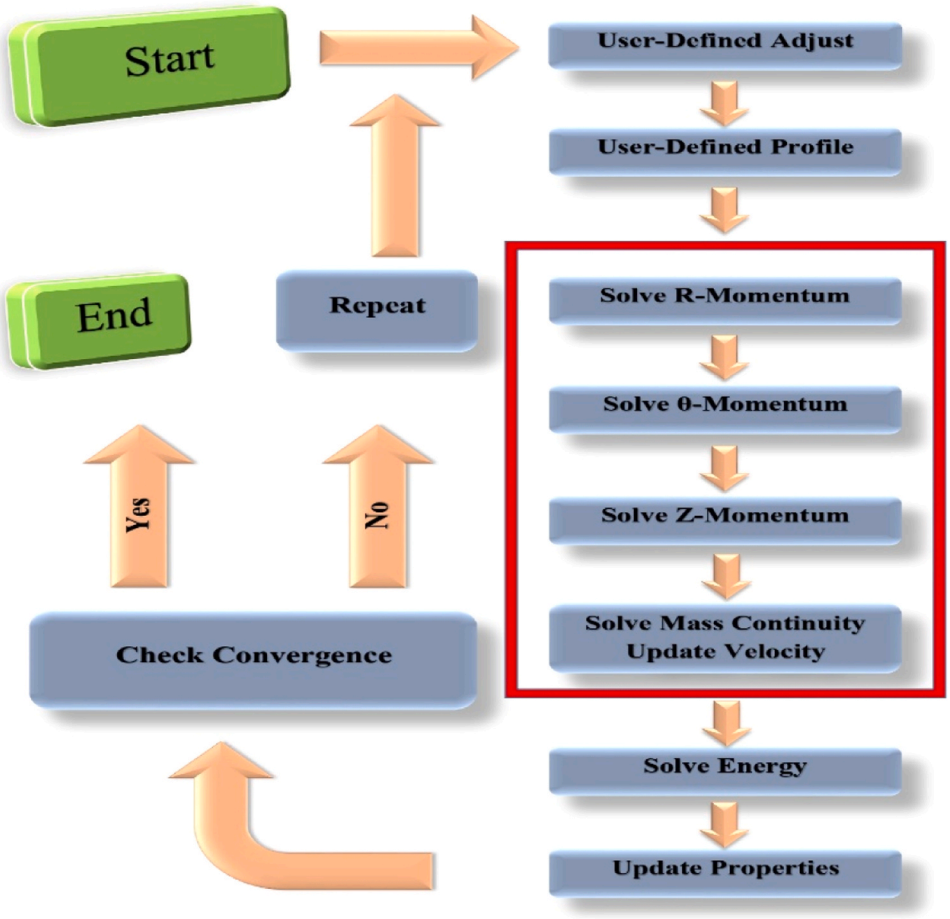

Fig. 2. The method of solving the governing equations [54].

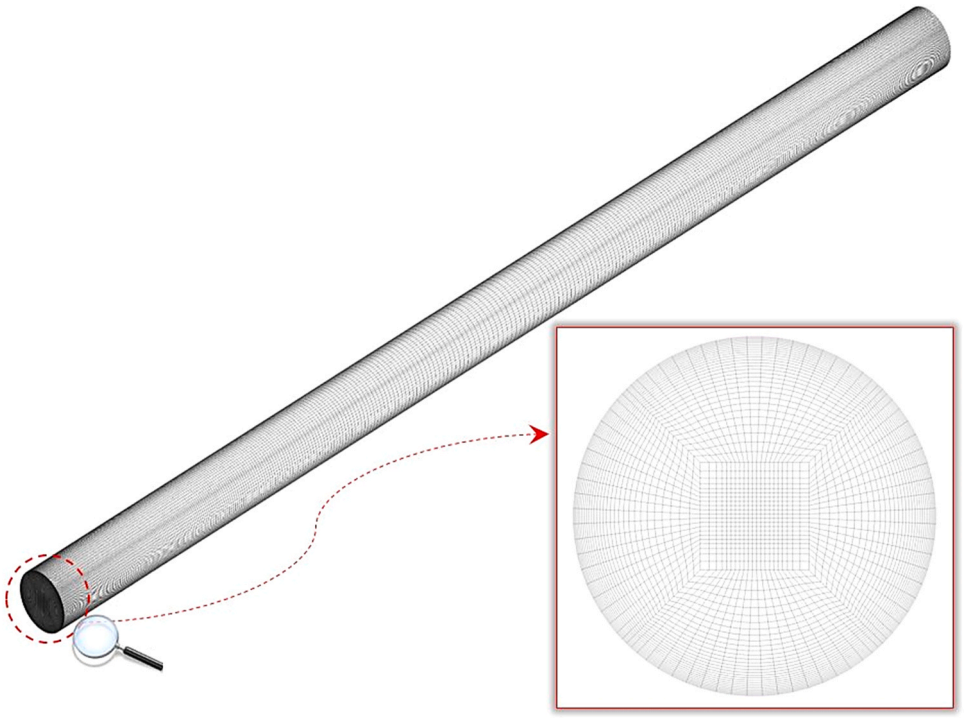

Fig. 3. Grid generation for the proposed tube.

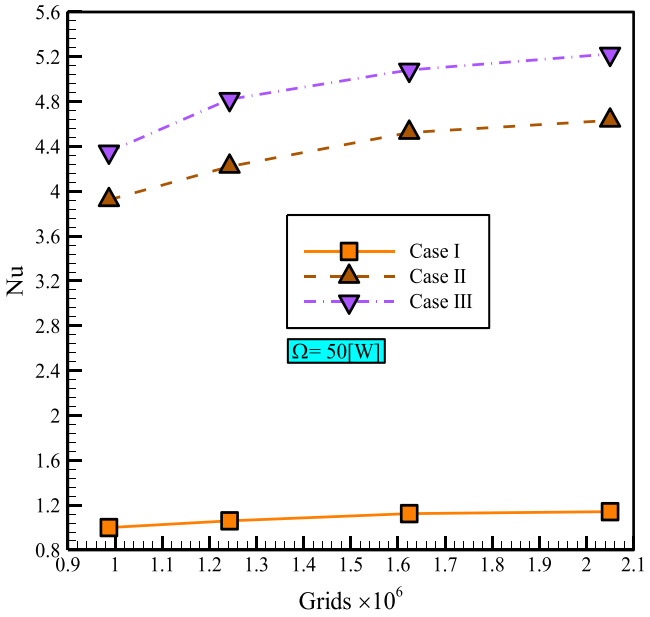

Fig. 4. Variation of Nusselt number at different elements number.

$$U = \frac{\omega H^2}{\alpha_f} \tag{32}$$

Where:

$$\alpha_f = \frac{k_f}{(\rho C_p)_f} \tag{33}$$

The magnitude of the velocity consists of three parts: the input velocity, the velocity due to the turbulent intensity of flow, and the velocity due to the circular motion of the magnetic field. The velocity parameter is implicit in the pumping power. However, the numerical definition of pumping power is defined [53]:

$$\Omega = \Delta P_L . V \tag{34}$$

where the pumping power Ω is in terms (W), the average pressure differenceΔP_L is in terms(Pa) and the magnitude of the velocity V is in terms $\left(\frac{m}{s}\right)$.

2.3. Boundary conditions

- No-slip condition on the wall is as follow and (z, r, θ) are the cylindrical coordinates:

$$\begin{cases} V_r(z, r_0) = 0 \\ V_\theta(z, r_0) = 0 \\ V_z(z, r_0) = 0 \end{cases} \tag{35}$$

- Inlet velocity:

$$\begin{cases} V_r(0, r) = 0 \\ V_z(0, r) = V_{in} \\ V_\theta(0, r) = 0 \end{cases} \tag{36}$$

$$\begin{cases} T(z, r_0) = T_w \\ T(0, r) = T_{in} \end{cases} \begin{cases} T|f = T|_w \\ k_m \dfrac{\partial T}{\partial r}\Big|f = k_m \dfrac{\partial T}{\partial r}\Big|_w \end{cases} \tag{37}$$

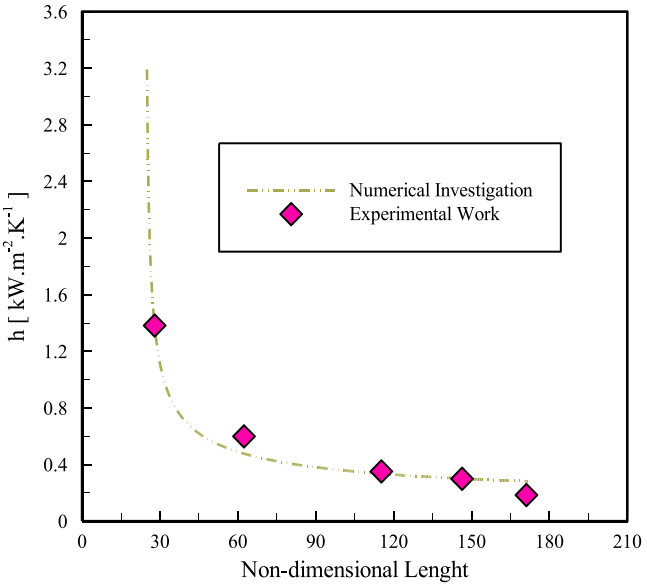

Fig. 5. Validation result of the present research with Experimental study [51].

2.4. Numerical simulation

In the present simulation, the thermo-fluid behavior of a tube containing Ag/water nanofluid under a rotational MF with different velocities have been investigated. The SIMPLE method and the finite volume approach have employed for a couple of velocity and pressure solution. The double-precision formulations and the second-order upwind equations variables have been utilized to solve the energy, momentum, and mass formulations accurately. Fig. 2. depicts the flowchart of solving the governing equations.

2.5. Grid generation, sensitivity analysis, and validation

The generated mesh for the proposed tube in this research is shown in Fig. 3. The grid sensitivity results of the present research for three cases at 50 W pump power are demonstrated in Fig. 4. According to the findings, promoting the number of elements leads to less error between Nusselt numbers. To reduce the cost of the calculation and save time, the appropriate number of elements was taken into account for this simulation. Additionally, the quantity of the CHTC variations along the entire length of the tube in the current research has been validated with the empirical work of Wen et al. [51] to guarantee the accuracy of the outcomes. The present outcomes and Wen et al.'s [51] findings have a good degree of consistency, as shown in Fig. 5. The graph of y^+ shows that the value of y^+ starts from low values located on the wall and reaches high values with distance from the walls. By investigating the Fig. 6 and according to the turbulence model used in this study, we conclude that since the value of y^+ near the wall is between 0 and 1 and generally in the other parts of the grid is below 5, the grid used is fine enough and the accuracy of the solution is confirmed.

3. Results and discussions

In the current research, the effect of employing a magnetic field in three cases, i.e., Case I: static and motionless MF, Case II: rotating MF with fixed dimensionless velocity, and Case III: rotating MF with twice the velocity of the Case II, on a tube including Ag/water nanofluid, are simulated applying the two-phase mixture model. Fig. 7 demonstrates the Nu number variations at various pump power for water and Ag/water nanofluid with 0.5 % volume fraction for three cases. Nusselt number increases by improving pump power for three cases and two types of working fluids. The Nu number is the proportion of the

Fig. 6. y^+ contour.

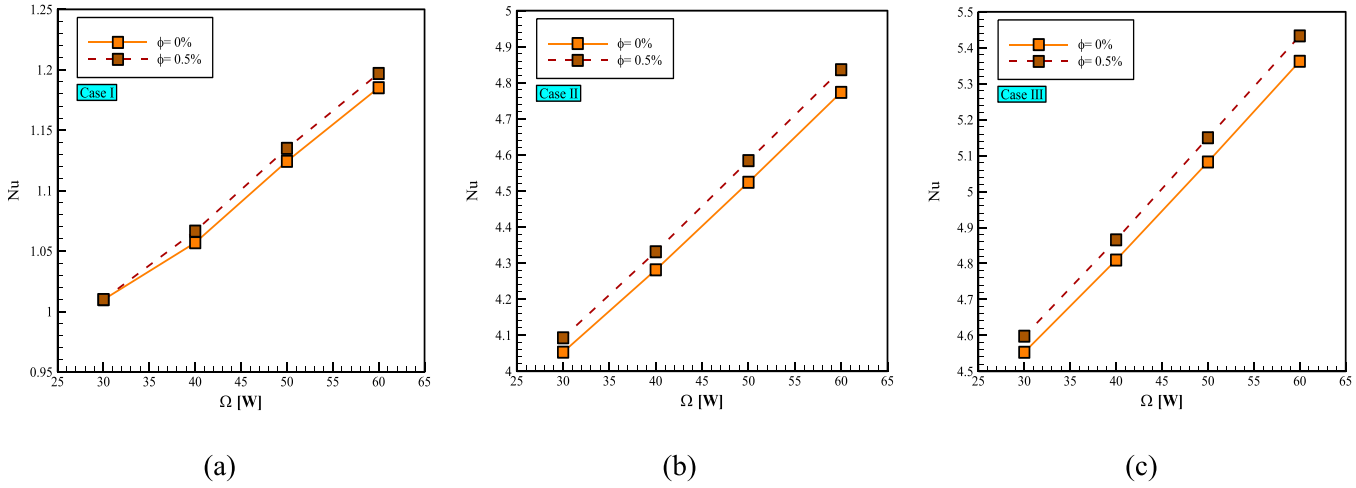

Fig. 7. Nusselt number changes at different pump powers.

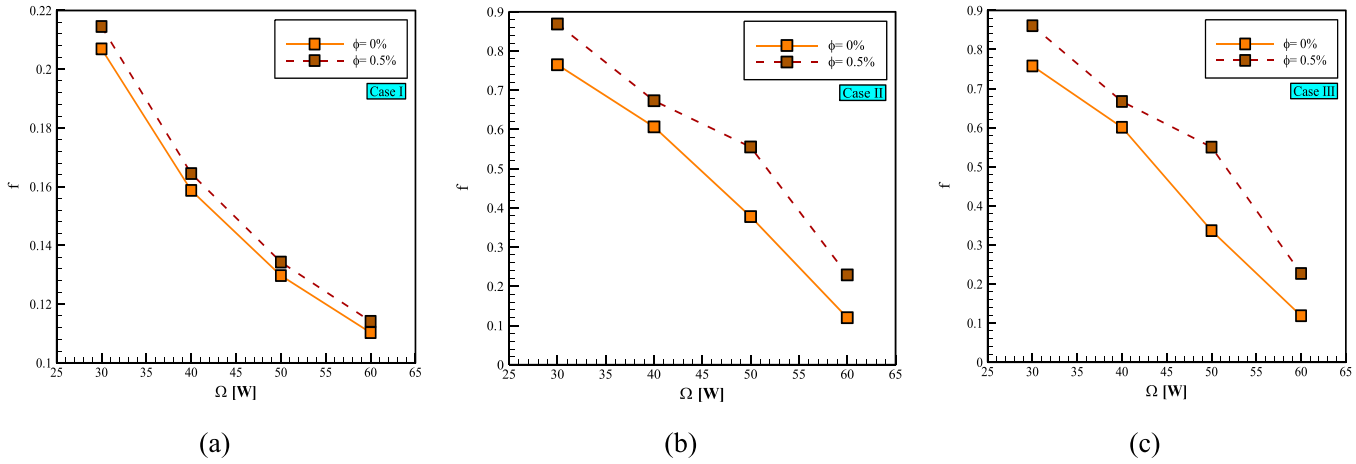

Fig. 8. Friction factor variations at different pump powers.

convection over the conduction. When the power improves, the enhancement of the mass flow rate leads to the convection improvement that leads to the Nusselt number enhancement. Moreover, adding Ag nanoparticles to the water leads to the Nu number enhancement. For Case III, the maximum Nu number was derived at 0.5 % Ag/water nanofluid and a power of 60 W. The rotating magnetic field for the Case III in comparison to the Case I and Case II at 60 W and 0.5 % volume fraction of nanofluid, enhanced the Nusselt number by 356.3 % and 12.42 %, respectively. The turbulence intensity of flow increases and according to the fluctuations created in the fluid, the heat transfer rate and Nusselt number increase. Also, by comparing between cases 1 and 3, it is clear that increasing the rotational speed of the magnetic field has an increasing effect on the fluctuations and turbulence intensity of flow and increases Nusselt.

Based on Eq. (20), the friction factor has an inverse relation with inlet velocity. By enhancing the power of pumping, the rate of mass flow and consequently the inlet velocity are enhanced. Thus, the friction factor declines with improved power. As shown in Fig. 8, the friction factor was reduced by improving the pump power. Also, using a 0.5 % volume fraction of Ag/water nanofluid as a working fluid increases the friction factor compared to water. Moreover, the factor of friction variations for Case II and Case III are the same. It seems that rotating

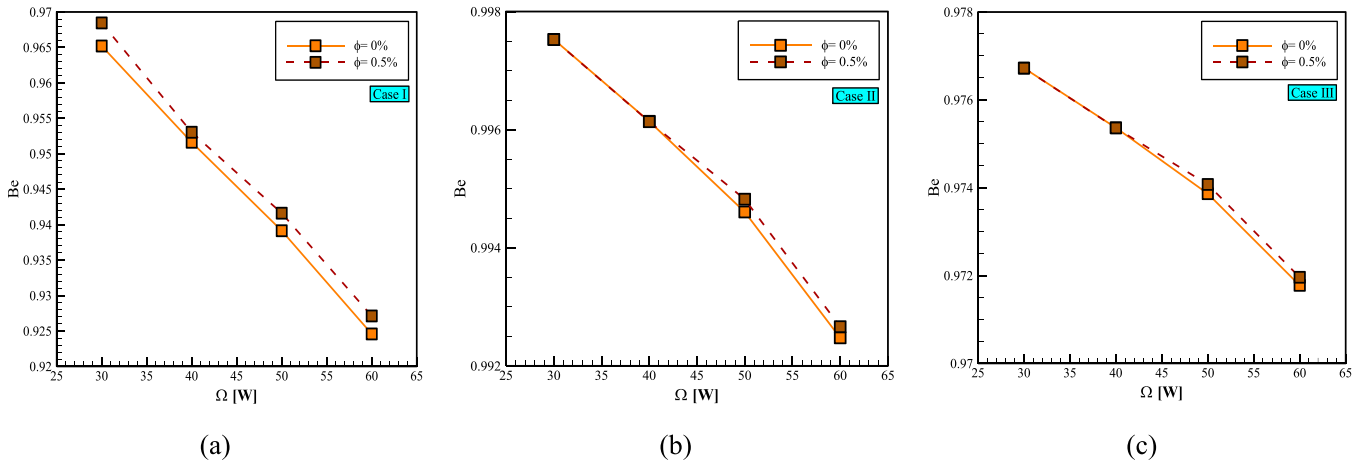

Fig. 9. Variation of Bejan number at different pump powers.

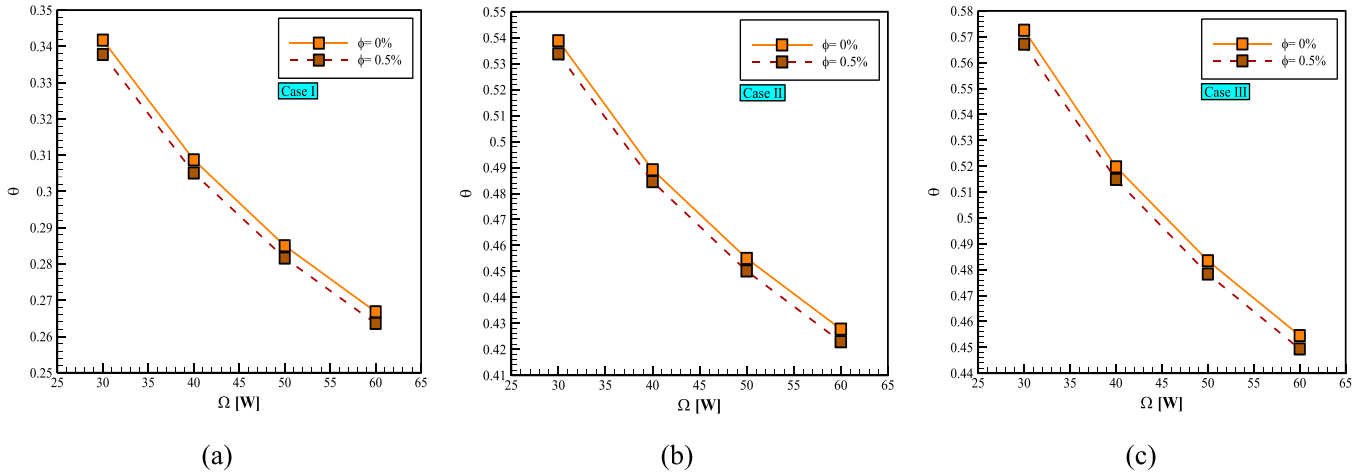

Fig. 10. Changes in dimensionless temperature at different pump powers.

magnetic field velocity doesn't affect the factor of friction, significantly. However, the amount of factor of friction increased by 103.5 % for Case II and Case III by using 60 W power pump and 0.5 % nanofluid compared to Case I. As we know from the mechanics of fluids and flow inside the pipes and channels, with the increase in velocity and momentum of the flow, the flow regime will move towards complete turbulence and the friction coefficient will decrease. With the movement of the fluid flow inside the pipe or channel, the amount of shear stress and friction force, and as a result, f factor decreases.

As presented in Eq. (25), Be number is the thermal entropy generation over the total entropy generation that demonstrates thermodynamic irreversibility. In the current research, by enhancing the pump power and mass flow rate, the Be number was reduced in three cases. The gradual expansion of the thermal boundary layer and the raise in

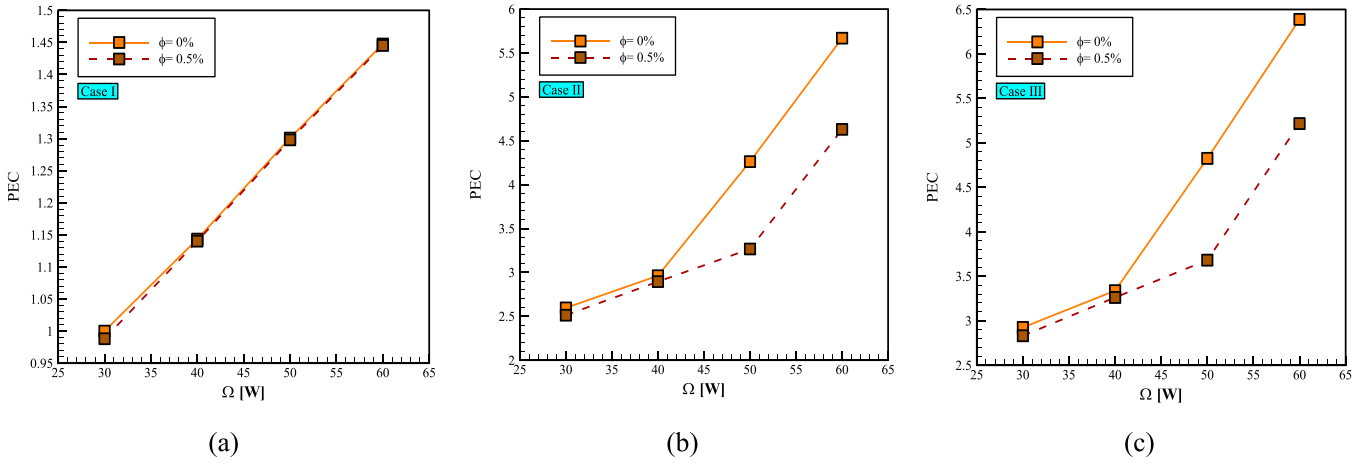

Fig. 11. The PEC outcomes at different pump powers.

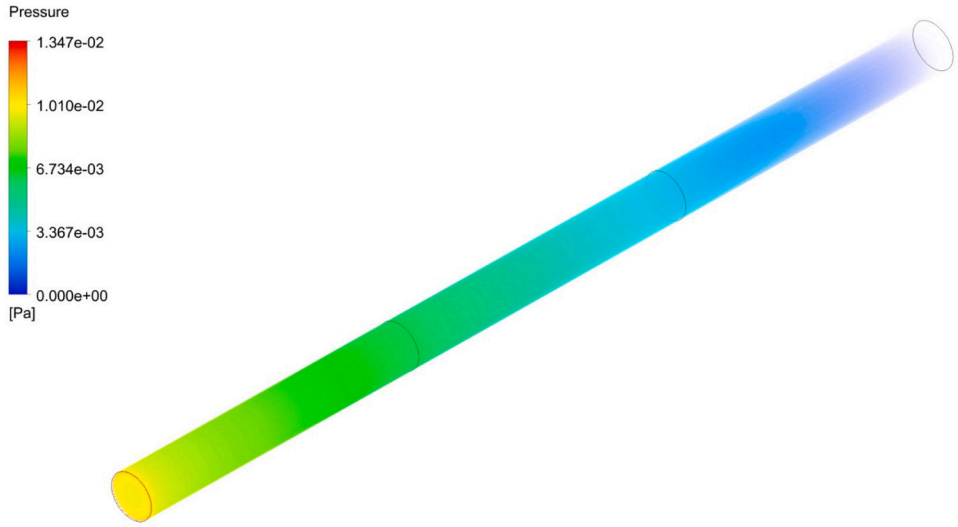

(a)

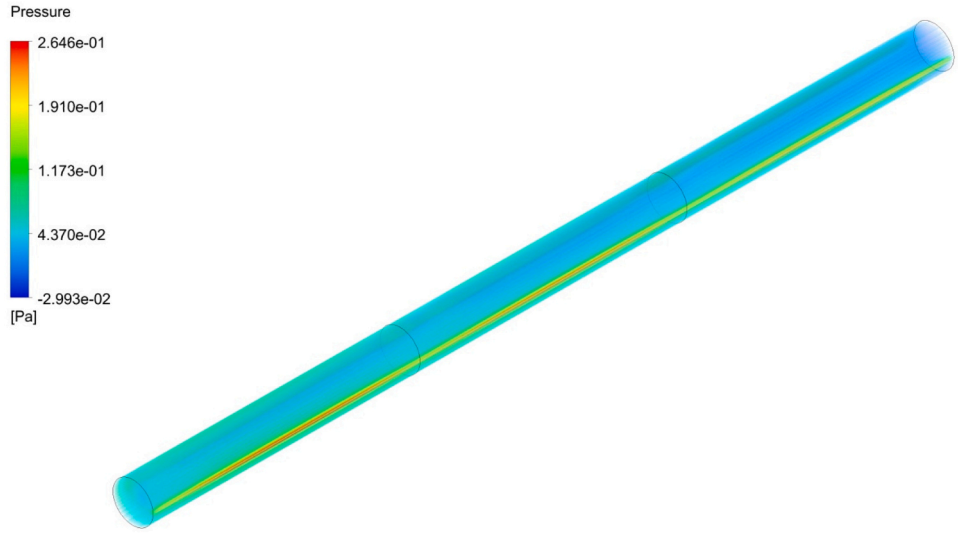

(b)

Fig. 12. Pressure variation contours; a) Case I, b) Case III.

velocity are the reasons of this phenomenon. The downward trend of the Be number is similar to the thermal entropy generated due to its dominance and the negligibility of frictional entropy generation. As shown in Fig. 9 using nanofluid generates more entropy generation, and the Be number increases by adding Ag nanoparticles to the water; although, this increment is more explicit for Case I. The maximum and minimum entropy generation were obtained at 30 W and 60 W pump power for Case II and Case I, respectively. As we know from the second law of thermodynamics, with increasing velocity and increasing flow disturbances, entropy increases and directs the flow towards greater irreversibility. From the Fig. 9 and Eq. (25), it can be seen that the amount of entropy produced by the magnetic field in the denominator of the fraction grows at a higher rate than the entropy produced by heat transfer in the numerator of the fraction, as a result, Bejan has a downward trend.

Fig. 10 illustrates the dimensionless temperature in terms of pump power of two working fluids for three Cases. By raising mass flow rate and pump power, the working fluid's velocity raises significantly, which raises the Reynolds number. By raising the Re number in a tube, the amount of time needed for heat to transfer from the fluid to the inner part of wall minimizes and as a result the dimensionless temperature was reduced. As demonstrated in Fig. 10, improving the pump power leads to the dimensionless temperature reduction. Also, utilizing nanofluid reduces the dimensionless temperature in compare with water base fluid. Moreover, static and motionless magnetic field has a substantially lower dimensionless temperature in compare with rotating MF (case II), and enhancing the rotational velocity of MF (case III) improve the dimensionless temperature about 6.66 % by using 60 W power pump and 0.5 % nanofluid. The highest dimensionless temperature obtained 0.575 for Case III at power of 30 W by using water. As the flow velocity increases by enhancing the pump power, it can be seen that the amount of heat exchange between the surface and the fluid decreases and according to the definition of θ and the almost constant wall temperature, the fluid temperature will decrease and θ will have a downward trend.

PEC is an index to show the best efficiency and performance of the system. Fig. 11 demonstrates the PEC in terms of pump power for three Cases using water and nanofluid. The diagrams display upward trend for two types of working fluids while the amount of increment is more

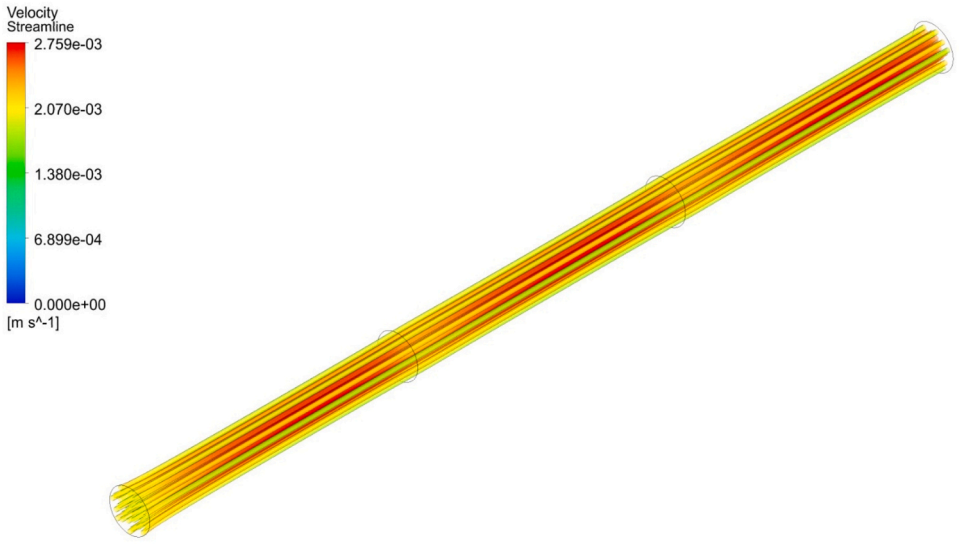

(a)

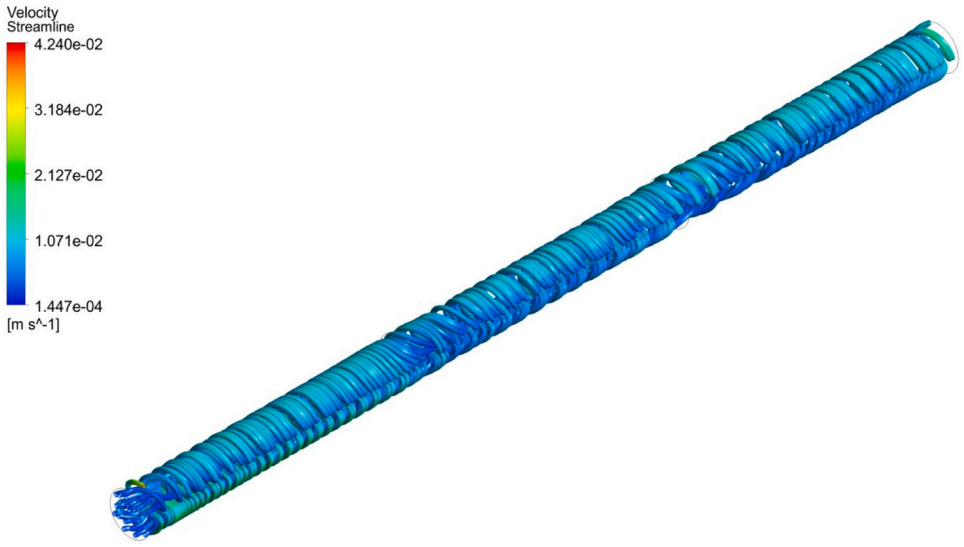

(b)

Fig. 13. Velocity streamline contours; a) Case I, b) Case III.

significant for Case II and Case III. Improving the pump power leads to the PEC improvement for three cases. Overall, using water as a working fluid makes better performance for the proposed system, precisely in Case III and Case II, however, both working fluids have the same performance in Case I. Moreover, compared to Case I, rotating magnetic field at 60 W and 0.5 % volume fraction of nanofluid improved the PEC about 219.44 % and 261.11 % for Case II and Case III, respectively. To add, by comparing the figures of f and Nu, it can be seen that between cases II and III at a constant pump power, the increase in Nusselt number was much more significant than f. Furthermore, according to the PEC equation (Eq. (26)), the increase in the numerator of the fraction compared to the increase in the denominator of the fraction as a result of the increase in the speed of the magnetic field is much more significant, so PEC is always more than 1 in this problem.

Flow physics are shown in Figs. 12–15 for 0.5 % volume fraction of Ag/water nanofluid at 60 W pump power for Case I and Case III. The pressure distribution is demonstrated in Fig. 12. It is explicitly demonstrated that nanofluid pressure distribution under rotating magnetic field increase across the whole length of the tube. Fig. 13 display the velocity streamline of nanofluid for Case I and Case III. As observed in Fig. 13, the nanofluid follows the same course across the whole length of the tube in Case I, however, nanofluid flow path under rotating magnetic field alter and leads to the flow rotation in Case III. Also, according to the Fig. 14, the rotating magnetic field improve the velocity. Fig. 15 represents the temperature distribution of nanofluid in Case I and Case III. Since the nanofluid velocity enhancement under rotating MF minimizes the amount of time needed for heat to transfer from the fluid to the inner part of the wall, the temperature is decreased.

To better usage of this study's results, a mathematical correlation was performed between Ω, Be, and Nu in all three cases and for two volume fractions of 0 % and 0.5 %. The results are shown in Table 2 and have a high accuracy of 97 %.

4. Conclusion

The main novelty of this paper is the thermofluidic characteristics and entropy generation in a tube with nanofluid under an altering rotatable magnetic field. So, this study evaluates the impact of rotating MF in two velocities on a tube including two types of working fluid namely 0.5 % volume fraction of Ag/water nanofluid and water using

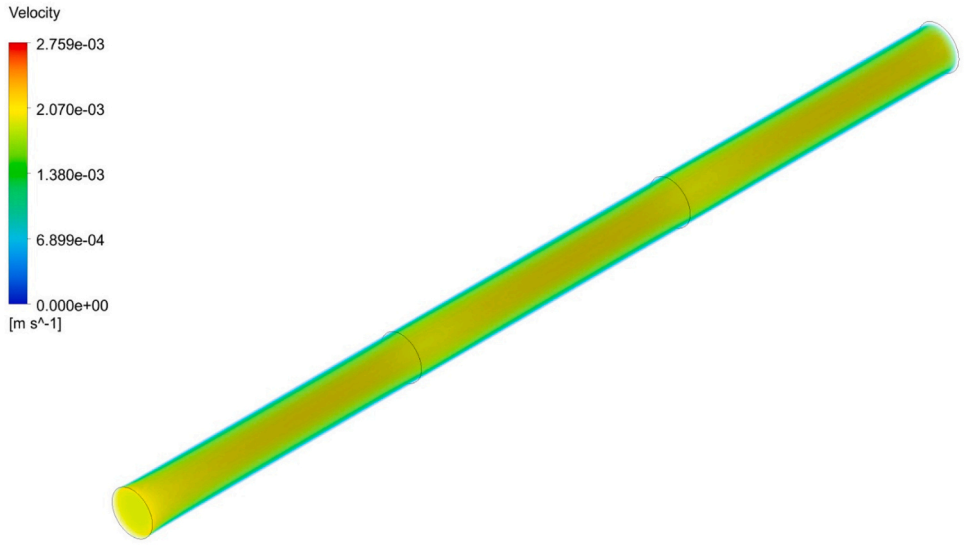

(a)

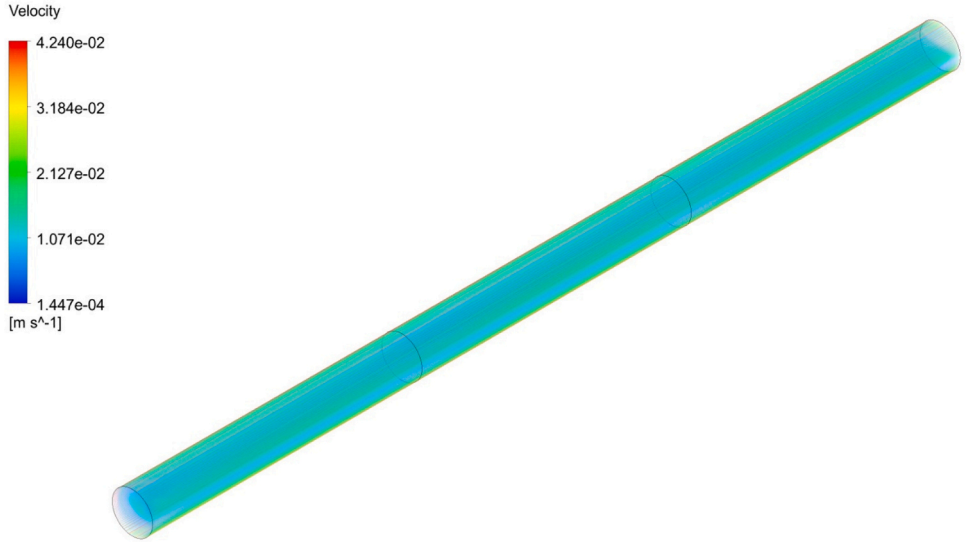

(b)

Fig. 14. Velocity variation contours; a) Case I, b) Case III.

mixture model at four pump power, i.e., 30 W, 40 W, 50 W, and 60 W. The following facts are obtained from present investigation.

- The rotating magnetic field for the Case III in comparison to the Case I and Case II at 60 W and 0.5 % volume fraction of nanofluid, enhanced the Nusselt number by 356.3 % and 12.42 %, respectively.
- Nusselt number enhances by improving pump power for three cases and two types of working fluids. This enhancement is more significant for Case III by using nanofluid.
- According to the Performance Evaluation Criteria (PEC) results, utilizing water as a working fluid has better performance for the proposed system, precisely in Cases II and III. In comparison to Case I, rotating magnetic field at 60 W and 0.5 % volume fraction of nanofluid improved the PEC about 219.44 % and 261.11 % for Case II and Case III, respectively.
- The static and motionless magnetic field has a substantially lower dimensionless temperature in compare with rotating MF (case II), and enhancing the rotational velocity of MF (case III) improve the dimensionless temperature about 6.66 %. The highest dimensionless temperature obtained 0.575 for Case III at power of 30 W by using water.
- Increasing the pump power leads to the dimensionless temperature reduction. Aditionally, utilizing nanofluid reduces the dimensionless temperature in compare with water base fluid.
- The friction factor declines by improving the pump power and using nanofluid enhance the friction factor compared to the water.
- By increasing the pump power and mass flow rate, Bejan number declines for three cases. The maximum and minimum entropy generation derived at 30 W and 60 W pump power for Case II and Case I, respectively.

CRediT authorship contribution statement

Mohammad Akbari: Supervision, Writing – original draft. **Saeed Amir Mohammadahmadi:** Resources, Visualization. **Hamidreza Azimy:** Software, Writing – original draft. **Shahab Naghdi Sedeh:** Investigation, Methodology. **Noushin Azimy:** Data curation, Formal analysis. **Mohammad Hossein Razavi Dehkordi:** Conceptualization,

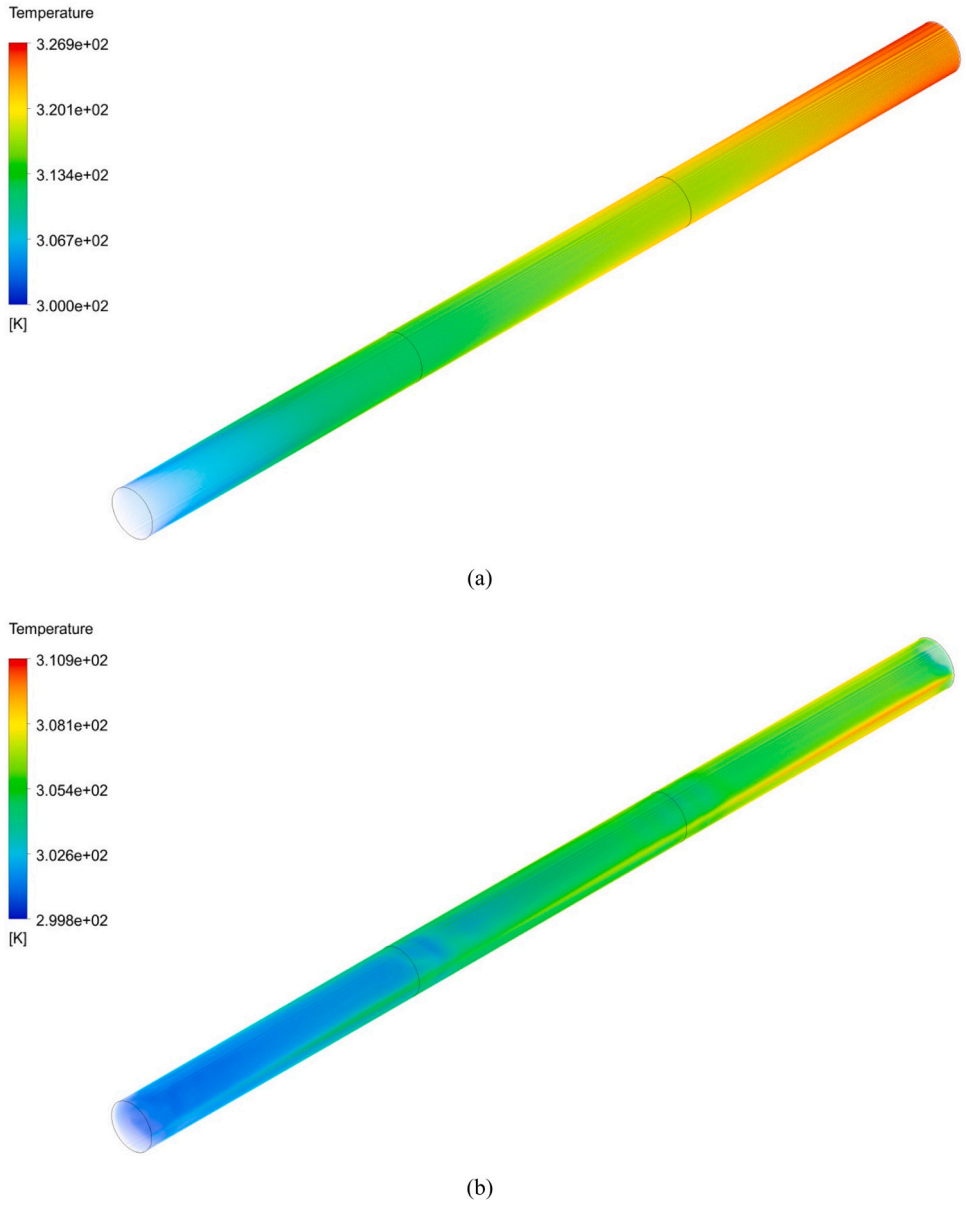

Fig. 15. Temperature variation contours; a) Case I, b) Case III.

Table 2
Mathematical correlation equations.

Case **I**	φ=0 %	$\Omega = 1133–1150\times Be - 616.5\times Nu + 592.9\times Be\times Nu + 50.84\times Nu\hat{}2$
	φ=0.5 %	$\Omega = 249.9–338.7\times Be + 46.95\times Nu + 65.7\times Be\times Nu - 3.469\times Nu\hat{}2$
Case **II**	φ=0 %	$\Omega = -9833 + 9397\times Be + 2230\times Nu - 2045\times Be\times Nu – 17.09\times Nu\hat{}2$
	φ=0.5 %	$\Omega = -3445 + 3171\times Be + 896.2\times Nu – 788.1\times Be\times Nu – 8.28\times Nu\hat{}2$
Case **III**	φ=0 %	$\Omega = -9833 + 9598\times Be + 1985\times Nu - 1859\times Be\times Nu – 13.54\times Nu\hat{}2$
	φ=0.5 %	$\Omega = -3445 + 3239\times Be + 797.8\times Nu – 716.4\times Be\times Nu – 6.561\times Nu\hat{}2$

Writing – original draft.

Declaration of Competing Interest

The authors declare that they have no known competing financial interests or personal relationships that could have appeared to influence the work reported in this paper.

References

[1] S. Li, F. Ali, A. Zaib, K. Loganathan, S.M. Eldin, M.I. Khan, Bioconvection effect in the Carreau nanofluid with Cattaneo–Christov heat flux using stagnation point flow in the entropy generation: Micromachines level study, Open Phys. vol. 21 (1) (2023).
[2] S. Li, M.I. Khan, F. Alzahrani, S.M. Eldin, Heat and mass transport analysis in radiative time dependent flow in the presence of Ohmic heating and chemical reaction, viscous dissipation: An entropy modeling, Case Stud. Therm. Eng. vol. 42 (2023) 102722.
[3] D. Wei, L. Lili, Y. Zhi, et al., Influence of nanoparticles on heat transfer characteristics of supercritical carbon dioxide fluid [J], Journal of Ordnance Equipment Engineering 44 (5) (2023) 142–149.
[4] Q. Chao, X. Wei, J. Tao, C. Liu, Y. Wang, Cavitation recognition of axial piston pumps in noisy environment based on Grad-CAM visualization technique, 2023/03/01, CAAI Trans. Intell. Technol. vol. 8 (1) (2023) 206–218, 2023/03/01.
[5] S. Nazia, B. Seshaiah, P. Sudarsana Reddy, P. Sreedevi, Silver–ethylene glycol and copper–ethylene glycol based thermally radiative nanofluid characteristics between two rotating stretchable disks with modified Fourier heat flux, Heat. Transf. vol. 52 (1) (2023) 289–316.

[6] P. Sreedevi, P. Sudarsana Reddy, M.A. Sheremet, Impact of homogeneous–heterogeneous reactions on heat and mass transfer flow of Au–Eg and Ag–Eg Maxwell nanofluid past a horizontal stretched cylinder, 2020/07/01, J. Therm. Anal. Calorim. vol. 141 (1) (2020) 533–546, 2020/07/01.

[7] Y. Yibo, X. Hui, Z. Yi, Study on heat transfer characteristics of high temperature heat pipe with large length diameter ratio [J], Journal of Ordnance Equipment Engineering 44 (10) (2023) 280–286.

[8] P.S. Reddy and A.J. Chamkha, HEAT AND MASS TRANSFER CHARACTERISTICS OF Al2O3−WATER AND Ag−WATER NANOFLUID THROUGH POROUS MEDIA OVER A VERTICAL CONE WITH HEAT GENERATION/ABSORPTION, vol. 20, no. 1, pp. 1-17, 2017-02-20 2017.

[9] H. Wang, et al., Magnetic field sensor using the magnetic fluid encapsulated long-period fiber grating inscribed in the thin-cladding fiber, 11/13, J. Opt. Photonics Res. (2023), 11/13.

[10] M.S. Babu, et al., Chemically reactive flow of viscous thermophoretic fluid over wedge with variable thermal conductivity and viscosity, Case Stud. Therm. Eng. vol. 45 (2023) 102924.

[11] S. Li, et al., Analysis of the Thomson and Troian velocity slip for the flow of ternary nanofluid past a stretching sheet, Sci. Rep. vol. 13 (1) (2023) 2340, 2023/02/09.

[12] Z. Liu, et al., Numerical bio-convective assessment for rate type nanofluid influenced by Nield thermal constraints and distinct slip features, Case Stud. Therm. Eng. vol. 44 (2023) 102821.

[13] P. Sudarsana Reddy, A.J. Chamkha, Influence of size, shape, type of nanoparticles, type and temperature of the base fluid on natural convection MHD of nanofluids, 2016/03/01/, Alex. Eng. J. vol. 55 (1) (2016) 331–341, 2016/03/01/.

[14] M. Ding, M. Tang, Z. Hua, X. Wang, Y. Zhao, Magnetic Field Sensing by Magnetic-Fluid-Coated Capillary Long-Period Fiber Gratings, J. Opt. Photonics Res. (2023), 11/22.

[15] Y. Peng, et al., Analysis of the effect of roughness and concentration of Fe3O4/water nanofluid on the boiling heat transfer using the artificial neural network: An experimental and numerical study, Int. J. Therm. Sci. vol. 163 (2021) 106863.

[16] F. Fan, C. Qi, J. Tu, Z. Ding, Effects of variable magnetic field on particle fouling properties of magnetic nanofluids in a novel thermal exchanger system, Int. J. Therm. Sci. vol. 175 (2022) 107463.

[17] S.V. Mousavi, M. Sheikholeslami, M.B. Gerdroodbary, The Influence of magnetic field on heat transfer of magnetic nanofluid in a sinusoidal double pipe heat exchanger, Chem. Eng. Res. Des. vol. 113 (2016) 112–124.

[18] M. Bezaatpour, M. Goharkhah, Convective heat transfer enhancement in a double pipe mini heat exchanger by magnetic field induced swirling flow, Appl. Therm. Eng. vol. 167 (2020) 114801.

[19] A. Shakiba, K. Vahedi, Numerical analysis of magnetic field effects on hydro-thermal behavior of a magnetic nanofluid in a double pipe heat exchanger, J. Magn. Magn. Mater. vol. 402 (2016) 131–142.

[20] Y. Ma, R. Mohebbi, M. Rashidi, Z. Yang, M. Sheremet, r thermal convection in I-shaped multiple-pipe heat exchanger under magnetic field influence, Phys. A: Stat. Mech. its Appl. vol. 550 (2020) 124028.

[21] S.E. Hosseinizadeh, S. Majidi, M. Goharkhah, A. Jahangiri, Energy and exergy analysis of ferrofluid flow in a triple tube heat exchanger under the influence of an external magnetic field, Therm. Sci. Eng. Prog. vol. 25 (2021) 101019.

[22] Y. Azizi, M. Bahramkhoo, A. Kazemi, Influence of non-uniform magnetic field on the thermal efficiency hydrodynamic characteristics of nanofluid in double pipe heat exchanger, Sci. Rep. vol. 13 (1) (2023) 407.

[23] J. Sodagar-Abardeh, P. Nasery, A. Arabkoohsar, M. Farzaneh-Gord, Numerical Study of Magnetic Field Influence on Three-Dimensional Flow Regime and Combined-Convection Heat Exchange Within Concentric and Eccentric Rotating Cylinders, J. Energy Resour. Technol. vol. 142 (11) (2020) 112115.

[24] Y.-M. Chu, R. Moradi, A.M. Abazari, Computational investigation of non-uniform magnetic field on thermal characteristic of nanofluid stream inside 1 8 0◦ elbow pipe, Mod. Phys. Lett. B vol. 35 (09) (2021) 2150157.

[25] A.A. Alnaqi, S. Aghakhani, A.H. Pordanjani, R. Bakhtiari, A. Asadi, M.-D. Tran, Effects of magnetic field on the convective heat transfer rate and entropy generation of a nanofluid in an inclined square cavity equipped with a conductor fin: Considering the radiation effect, Int. J. Heat. Mass Transf. vol. 133 (2019) 256–267.

[26] S. Hosseini, M. Sheikholeslami, Investigation of the nanofluid convective flow and entropy generation within a microchannel heat sink involving magnetic field, Powder Technol. vol. 351 (2019) 195–202.

[27] F. Selimefendigil, H.F. Öztop, Natural convection and entropy generation of nanofluid filled cavity having different shaped obstacles under the influence of magnetic field and internal heat generation, J. Taiwan Inst. Chem. Eng. vol. 56 (2015) 42–56.

[28] M. Bahiraei, M. Hangi, Investigating the efficacy of magnetic nanofluid as a coolant in double-pipe heat exchanger in the presence of magnetic field, Energy Convers. Manag. vol. 76 (2013) 1125–1133.

[29] Y. Khetib, A.A. Alahmadi, A. Alzaed, A. Tahmasebi, M. Sharifpur, G. Cheraghian, Natural convection and entropy generation of MgO/water nanofluids in the enclosure under a magnetic field and radiation effects, Processes vol. 9 (8) (2021) 1277.

[30] S. Hariri, M. Mokhtari, M.B. Gerdroodbary, K. Fallah, Numerical investigation of the heat transfer of a ferrofluid inside a tube in the presence of a non-uniform magnetic field, Eur. Phys. J. vol. 132 (2017) 1–14.

[31] S. Safarzadeh, M. Niknam-Azodi, A. Aldaghi, A. Taheri, M. Passandideh-Fard, M. Mohammadi, Energy and entropy generation analyses of a nanofluid-based helically coiled pipe under a constant magnetic field using smooth and micro-fin pipes: Experimental study and prediction via ANFIS model, Int. Commun. Heat. Mass Transf. vol. 126 (2021) 105405.

[32] A. Chamkha, M. Ismael, A. Kasaeipoor, T. Armaghani, Entropy generation and natural convection of CuO-water nanofluid in C-shaped cavity under magnetic field, Entropy vol. 18 (2) (2016) 50.

[33] Z. Shah, M. Sheikholeslami, P. Kumam, Influence of nanoparticles inclusion into water on convective magneto hydrodynamic flow with heat transfer and entropy generation through permeable domain, Case Stud. Therm. Eng. vol. 21 (2020) 100732.

[34] F. Selimefendigil, H.F. Öztop, A.J. Chamkha, MHD mixed convection and entropy generation of nanofluid filled lid driven cavity under the influence of inclined magnetic fields imposed to its upper and lower diagonal triangular domains, J. Magn. Magn. Mater. vol. 406 (2016) 266–281.

[35] D.Y. Aydın, E. Aydin, M. Gürü, The effects of particle mass fraction and static magnetic field on the thermal performance of NiFe2O4 nanofluid in a heat pipe, Int. J. Therm. Sci. vol. 183 (2023) 107875.

[36] M.J.P. Razzaghi, M. Asadollahzadeh, M.R. Tajbakhsh, R. Mohammadzadeh, M.Z. M. Abad, E. Nadimi, Investigation of a temperature-sensitive ferrofluid to predict heat transfer and irreversibilities in LS-3 solar collector under line dipole magnetic field and a rotary twisted tape, Int. J. Therm. Sci. vol. 185 (2023) 108104.

[37] F. Selimefendigil, H.F. Öztop, Combined effects of using multiple porous cylinders and inclined magnetic field on the performance of hybrid nanoliquid forced convection, J. Magn. Magn. Mater. vol. 565 (2023) 170137.

[38] M. Mehrali, et al., Heat transfer and entropy generation analysis of hybrid graphene/Fe3O4 ferro-nanofluid flow under the influence of a magnetic field, Powder Technol. vol. 308 (2017) 149–157.

[39] A. Hajatzadeh Pordanjani, S. Aghakhani, A. Karimipour, M. Afrand, M. Goodarzi, Investigation of free convection heat transfer and entropy generation of nanofluid flow inside a cavity affected by magnetic field and thermal radiation, 2019/08/01, J. Therm. Anal. Calorim. vol. 137 (3) (2019) 997–1019, 2019/08/01.

[40] H. Aminfar, M. Mohammadpourfard, Y.N. Kahnamouei, Numerical study of magnetic field effects on the mixed convection of a magnetic nanofluid in a curved tube, Int. J. Mech. Sci. vol. 78 (2014) 81–90.

[41] Y. Ma, R. Mohebbi, M. Rashidi, Z. Yang, M.A. Sheremet, Numerical study of MHD nanofluid natural convection in a baffled U-shaped enclosure, Int. J. Heat. Mass Transf. vol. 130 (2019) 123–134.

[42] I. Fersadou, H. Kahalerras, M. El Ganaoui, MHD mixed convection and entropy generation of a nanofluid in a vertical porous channel, Comput. Fluids vol. 121 (2015) 164–179.

[43] M. Sheikholeslami, D.D. Ganji, M.Y. Javed, R. Ellahi, Effect of thermal radiation on magnetohydrodynamics nanofluid flow and heat transfer by means of two phase model, J. Magn. Magn. Mater. vol. 374 (2015) 36–43.

[44] A. Kabeel, E.M. El-Said, S. Dafea, A review of magnetic field effects on flow and heat transfer in liquids: present status and future potential for studies and applications, Renew. Sustain. Energy Rev. vol. 45 (2015) 830–837.

[45] M. Hadavand, S. Yousefzadeh, O.A. Akbari, F. Pourfattah, H.M. Nguyen, A. Asadi, A numerical investigation on the effects of mixed convection of Ag-water nanofluid inside a sim-circular lid-driven cavity on the temperature of an electronic silicon chip, Appl. Therm. Eng. vol. 162 (2019) 114298.

[46] T. Rahim, J. Hasnain, N. Abid, Z. Abbas, Entropy generation for mixed convection flow in vertical annulus with two regions hydromagnetic viscous and Cu-Ag water hybrid nanofluid through porous zone: a comparative numerical study, Propuls. Power Res. vol. 11 (3) (2022) 401–415.

[47] S.-L. Wang, X.-Y. Li, X.-D. Wang, G. Lu, Flow and heat transfer characteristics in double-layered microchannel heat sinks with porous fins, Int. Commun. Heat. Mass Transf. vol. 93 (2018) 41–47.

[48] L. Chuan, X.-D. Wang, T.-H. Wang, W.-M. Yan, Fluid flow and heat transfer in microchannel heat sink based on porous fin design concept, Int. Commun. Heat. Mass Transf. vol. 65 (2015) 52–57.

[49] N. Li, et al., Analysing thermal-hydraulic performance and energy efficiency of shell-and-tube heat exchangers with longitudinal flow based on experiment and numerical simulation, Energy vol. 202 (2020) 117757.

[50] A. Ebrahimi, F. Rikhtegar, A. Sabaghan, E. Roohi, Heat transfer and entropy generation in a microchannel with longitudinal vortex generators using nanofluids, Energy vol. 101 (2016) 190–201.

[51] D. Wen, Y. Ding, Experimental investigation into convective heat transfer of nanofluids at the entrance region under laminar flow conditions, Int. J. Heat. Mass Transf. vol. 47 (24) (2004) 5181–5188.

[52] F. Selimefendigil, H.F. Öztop, Mixed convection of nanofluids in a three dimensional cavity with two adiabatic inner rotating cylinders, Int. J. Heat. Mass Transf. vol. 117 (2018) 331–343.

[53] Y. Cengel, J. Cimbala, Ebook: Fluid Mechanics Fundamentals and Applications (si units), McGraw Hill, 2013.

[54] P. Barnoon, D. Toghraie, Numerical investigation of laminar flow and heat transfer of non-Newtonian nanofluid within a porous medium, Powder Technol. vol. 325 (2018) 78–91.